Received: January 28, 2024. Revised: February 28, 2024.

International Journal of
Intelligent Engineering & Systems

http://www.inass.org/

Brain Tumor Segmentation and Classification Using Binomial Thresholding-Based Bidirectional-Long-Short Term Memory

J. Shreeharsha[1]*

[1]*Department of Computer Science and Engineering, Rao Bahadur Y. Mahabaleswarappa Engineering College, Ballari, India*
* Corresponding author's Email: shreeharsharevanth9@gmail.com

Abstract: A brain tumor arises when abnormal cells develop in the brain, leading to an elevated risk of illness and mortality due to the accelerated growth of these tumor cells. Magnetic resonance imaging (MRI) is utilized for detecting and diagnosing brain tumors by providing images of the brain's internal structure. However, brain tumors lead to the death of numerous lives due to inaccurate segmentation and classification of brain tumors. In this research, the binomial thresholding-based bidirectional-long-short term memory (BT-Bi-LSTM) is proposed for accurate segmentation and classification. Initially, the image is acquired from BRATS 2019 and BRATS 2020 datasets and then normalization and contrast limited adaptive histogram equalization (CLAHE) approaches are established in pre-processing. The BT technique is employed for segmenting tumor portions from the pre-processed images. The gray-level Co-occurrence matrix (GLCM) and local ternary pattern (LTP) are employed to extract the features. Finally, the Bi-LSTM is used to classify the types of brain tumors. The BT-Bi-LSTM achieves better accuracy, precision, recall, and f1-score of 99.76%, 99.52%, 99.31%, and 98.69% for BRATS 2019 dataset compared to the existing approaches like DNN-based mathematical approach, tumor localization enhancement approach and U-net architecture, and Hybrid Convolution Neural Network (HCNN). When compared to tumor localization enhancement approach and U-net architecture, CNN, hybrid Deep CNN with k-means clustering, and 2D U-net, the BT-Bi-LSTM achieves better accuracy, precision, and recall of 99.89%, 99.76%, and 99.62% for BRATS 2020 dataset respectively.

Keywords: Binomial thresholding, Classification, Magnetic resonance imaging, Segmentation, Bidirectional-long-short term memory.

1. Introduction

The brain tumor is one of the deadly cancerous diseases that cause abnormal cells in the human brain [1]. The brain is the core and intricate organ of the human body that contains tissue and nerve cells to manage the activities of the whole body such as muscle movement and breathing [2, 3]. Due to the different tumor shapes and sizes, accurately identifying brain tumors before the remedy is challenging. Moreover, treatment is established by the stage and tumor types [4]. A brain tumor is categorized as a malignant or benign and a benign brain tumor is a slow-growing brain tumor and a malignant is a fast-growing tumor. MRI is a significant tool for the monitoring, diagnosis, and detection of brain tumors [5]. MRI is a popular non-intrusive imaging technique that produces a sensitive contrast between tissues [6, 7]. The MRI information is utilized to identify and classify the types of tumors like meningiomas, gliomas, and pituitary tumors to help doctors avoid risky histology processes [8]. The primary common kind of brain tumor is gliomas. The term "Glioma" is used to describe tumors that develop in brain structures other than blood vessels and nerve cells. Gliomas are separated into four groups: Grades 1 and 2 are considered low-grade tumors whereas grades 3 and 4 are considered high-grade tumors by the world health organization (WHO) [9].

Tumor cells from other parts of the human body can be transferred to the brain tissue through the

bloodstream, leading to the formation of established tumors known as secondary tumors.

There are two categories of brain tumors: primary and secondary. The tumor originating in the brain tissue is known as a primary tumor. Tumor cells from other parts of the body can be transferred to brain tissue through the bloodstream which is known as secondary tumors [10]. The MRI has four popular techniques: T1, T2, T3, and FLAIR to maximize cancer localization and classification accuracy [11]. An abnormal cell group grows within the brain or over the brain leading to brain tumors. Those cell groups affect the normal process of brain activity and demolish healthy cells [12]. Segmentation and classification are the primary phases in recognizing the brain tumor. The primary aim of the segmentation task is to locate the regions of tumor and non-tumor. Accurate segmentation is necessary to determine the size and location of a brain tumor. To separate an image into two pieces, imaging segmentation is utilized in the field of medical images. After the process of segmentation, the brain regions are recognized by the classification approach [13, 14]. Various approaches and algorithms are established for tumor segmentation because of the intricate segmentation procedure in the MRI image [15]. The primary contribution of this research is as follows:

- Two different approaches such as normalization and CLAHE are established to enhance the contrast and image's features by declaring the abnormal patterns and minimizing the noise. The BT approach is employed to segment the tumor portions from the images.
- For extracting the features, GLCM and LTP are established where GLCM is employed to obtain the data of statistics on a intensity of pixels, and LTP is utilized for extracting texture patterns.
- Finally, the Bi-LSTM is used to classify the brain tumor type effectively and accurately.

This paper is structured as follows: Section 2 presents a literature survey. The proposed technique is indicated in section 3. The results are represented in xection 4. Section 5 describes the conclusion.

2. Literature survey

The related works of this research are discussed along with their advantages and disadvantages.

Ajay S. Ladkat [16] presented a DNN-based mathematical approach for the segmentation of 3D brain tumors. Each slice of the 3D image was increased by the presented mathematical approach which was transmitted by the 3D attention U-Net to generate the outcome of segmented tumor. The presented approach provides accurate segmentation of tumor pixels from a 3D brain image. This approach maximizes the human lifetime and minimizes the amount of death by high accuracy and low complexity. However, this approach has limited memory and false tolerance.

Ahmet Ilhan [17] presented a tumor localization and enhancement approach and U-net architecture for the segmentation of brain tumors by employing MRI images. At first, histogram-based nonparametric tumor localization was employed to locate the region of a tumor and an enhancement technique was utilized to update the localized region to enhance the low-contrast or indistinct tumor visual appearance. The resultant images were passed through the U-net to segment the brain tumor. This approach generates greater accuracy and low-cost segmentation in the images of MRI. However, the FLAIR images consider only complete tumor segmentation not determining other modalities.

Arkapravo Chattopadhyay & Mausumi Maitra [18] implemented a convolutional neural network (CNN) for MRI-based brain tumor detection. The different MRI images were considered with different shapes, locations, the size of tumors, and various image intensities to perform the approach well. Moreover, the SVM classifier and activation approaches like sigmoid, SoftMax, and RMSProp were performed to cross-check the approach. The implemented CNN approach automatically learns challenging features from the MRI images of multi-modal. However, this approach has limitations such as time complexity and required weight optimization for different data fusion approaches.

B.V. Prakash [19] developed a hybrid CNN (HCNN) for brain tumor detection and classification. During the process of decomposition, the pixel stability was enhanced by a transform of Ridgelet, and then features were calculated from Ridgelet coefficient. Then, the features were categorized by utilizing HCNN, and a pixel of tumor was detected by employing a segmentation approach. This approach develops a complete computer-based automated technique for determining the images of meningioma and non-meningioma. However, HCNN faces challenges in interpretability due to a complexity of integrating various CNNs.

Akshya Kumar Sahoo [20] introduced a hybrid Deep CNN with k-means clustering for the segmentation of effective gliomas. The local center of mass (LCM) was utilized to segment the tumor core, whole tumor, and edema regions. Then, the k-means clustering was performed to extract edema

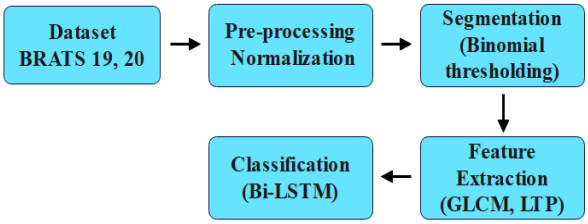

Figure. 1 Block diagram for the proposed technique

regions and tumor core. This approach achieves better performances in segmentation. However, this approach introduces additional hyperparameter tuning challenges due to hybrid techniques.

Sidratul Montaha [21] implemented an automated technique utilizing 2D U-net architecture for the segmentation of brain tumors. The 3D MRI's middle slice was automatically extracted and a normalization technique was performed. Then, the U-net was utilized to segment the brain tumor. The technique was validated and tested on four sequences which results in greater accuracy. However, this approach has difficulties in capturing the relationship of spatial in three-dimensional structure.

3. Proposed methodology

The BT-Bi-LSTM is proposed for brain tumor segmentation and classification. At first, an image is acquired from the brats 19 and 20 datasets, and two different approaches such as normalization and CLAHE are performed to enhance the data in pre-processing. Then, the BT approach is used for segmentation and GLCM and LTP are employed for feature extraction. Finally, the Bi-LSTM is utilized for brain tumor classification. Fig. 1. Indicates the block diagram for the proposed technique.

3.1 Datasets

The brain tumor segmentation and classification are analyzed using BRATS 2019 and BRATS 2020.

3.1.1. BRATS 2019

The BRATS 2019 dataset [22] has 335 cases with 76 occurrences of low-grade Glioma (LGG) and 259 occurrences of high-grade Glioma (HGG) accordingly. The testing and validation set includes 166 and 125 cases respectively. The ground truth images are manually established by utilizing the identical annotation protocol.

3.1.2. BRATS 2020

The BRATS 2020 [23] utilizes pre-operative MRI scans and focuses on segmentation. There are 369 training, 169 testing, and 125 validations in multimodal brain MRI. The training dataset contains 369 MRIs of which 76 are from LGG and 293 have been obtained from HGG for segmentation.

3.2 Pre-processing

The normalization and CLAHE are used in pre-processing which are explained below.

- The brain image's pixel intensity is increased by changing the limits of pixel by employing the normalization which is expressed in Eq. (1).

$$I' = (I - min)\frac{newmax - newmin}{max - min} + newmin \quad (1)$$

Where I represents the input image, max and min indicate maximum and minimum intensity values, and I' denotes the normalized image with $newmin$ and $newmax$ value of intensity.

- A CLAHE is used to enhance the contrast and image's features by declaring the abnormal patterns once the normalization is employed. It produces a realistic form among the family of histogram equalization and minimizes noise. The final pre-processed image is passed via segmentation procedure.

3.3 Segmentation using Binomial thresholding

After pre-processing, binomial thresholding is utilized for segmenting tumor portions from images. The segmentation of tumors in MRI is challenging due to the different factors like irregularity, and shape compared with the region of a healthy brain. The affected tumor segmentation image is more difficult than producing segmentation in the image of a healthy brain because of the ridiculous effects generated by the various tumor representations in the brain. To solve this problem, a binomial thresholding-based segmentation approach is performed. Segmentation is the primary significant phase in MRI analysis due to its evaluation of the modification in the brain, visualization and measuring of the structure of the anatomical brain, image-guided intervention, determination of pathological regions, and surgical planning. Here, the process of segmentation is developed depending on Binomial mean (BM), variance, and standard deviation (SD).

Let G denote the grey levels and the normalized image is expressed as $N_n(x, y)$ and the pixel's total number expression is denoted as $n = \sum_{a=0}^{G-1} I_a$ where the pixels at specific grey levels are represented as I_a.

The mathematical Eq. (2) is utilized to calculate each level's probabilities.

$$P_b = \frac{p(I_a)}{n} \tag{2}$$

The value of output obtained by this segmentation technique is in a logical form that contains two various classes, $C_{b=1} \epsilon \{0,1,2,\ldots.,t_1\}$ and $C_{b=2} \epsilon \{t_1+1,\ldots.L-1\}$ besides mean $\mu(t_1)$ and binomial variance $\sigma_c^2(t_1)$. Then, the mathematical formula is utilized to determine the cumulative probability $P_c(t_1)$ which is expressed in Eq. (3).

$$P_c(t_1) = 1 - P_{(c-1)(t_1)} \tag{3}$$

The variance and binomial mean for each class is represented in Eq. (4) and (5).

$$\beta_c(t_1) = \sum_{y=1}^{t_1} \frac{n!}{(y-1)!(n-y)!} P^y (1-P)^{n-y} \tag{4}$$

$$\sigma_c^2(t) = P_c(\mu_c(t_1) - \mu) + P_c(t_1)(\mu_c(t_1) - \mu) \tag{5}$$

Here, the value of the mean is expressed as $\beta = \sum_{a=1}^{n} \frac{p(N_a)}{n}$. The chosen criteria for the final value of the threshold are expressed in Eq. (6) and (7).

$$\tilde{\phi}^T = arg 0 \le t_1 \le G_{max} \sigma_r^2(t) \tag{6}$$

$$I_R(a,b) = I_n(a,b) \begin{cases} 1 \; if \; G \ge T \\ 0 \; if \; G < T \end{cases} \tag{7}$$

Where the $\tilde{\phi}^T$ denotes the threshold value, the binary image is expressed as $N_n(x,y)$, and the G represents gray-level pixels. After segmentation, feature extraction is performed to extract the features.

3.4 Feature extraction

After performing segmentation using binomial thresholding, GLCM, and LTP are employed for extracting features. GLCM is employed to obtain data of statistics and LTP is utilized for extracting the patterns of texture which is discussed below.

3.4.1. Grey-level co-occurrence matrix (GLCM)

The GLCM [24] is employed to determine the texture feature due to its increased accuracy. This determination is employed for maximizing the brain tumor's segmentation and classification. The GLCM evaluation is determined by input transfer depending on relationship of spatial between segmented images' pixel values. The pair of pixel values are established for producing a dependence matrix. Therefore, GLCM features like correlation data measures, entropy, inverse difference moment, and average of sum are utilized for establishing image's textural analysis.

3.4.2. Local ternary pattern (LTP)

LTP is [25] employed in the image processing as feature extraction. It is a Local Binary Pattern (LBP) extension in which the $s(z)$ function is expressed in Eq. (8).

$$s(z) = \begin{cases} 2 & if \; z \ge t \\ 1 & if \; |z| < t \\ 0 & if \; z \le -t \end{cases} \tag{8}$$

Where $z = g_p - g_c$ and t is the subject threshold. The LTP's primary coding is represented in Eq. (9).

$$LTP_{P,R} = \sum_{p=0}^{P-1} s(g_p - g_c) 3^p \tag{9}$$

The "greater than", "less than", and "equal" relationships conditions among pixel and neighbor are utilized for obtaining distinctive and sophisticated features. Then, the extracted features are passed into classification.

3.5 Classification

After feature extraction, the classification approach is utilized for the classification of brain tumors. Here, the Bi-LSTM approach is used to classify the tumor which is described below.

3.5.1. Long short-term memory (LSTM)

The LSTM generates numerous outcomes in domains like image processing and natural language processing (NLP). LSTM is a type of recurrent neural network (RNN) whjch learns long-term dependency as input features. The input gates, forget gates, and output gates are three gates of LSTM. The cell state and hidden state are two states which generates LSTM. At time t, the x_t and h_t are the input and the hidden state respectively. It has c_t cell state, and three gates which are i_t input gate, f_t forget gate, o_t output gate in the hidden state. The f_t evaluates how many rates it manages from the before value of cell state c_{t-1} at time t. The forget gate which is expressed in Eq. (10).

$$f_t = \sigma(U_f x_t + W_f h_{t-1} + b_f) \tag{10}$$

Where σ is the function of the sigmoid, W_f and U_f are the weight values and b_f is the bias value. The sigmoid function is utilized as an activation function by hyperbolic tangent function. In the neural network, the optimization approach like gradient descent is employed as a learning approach because they have differentiable functions. At time t, i_t input gate evaluates how much the processing output of x_t reflect the c_t cell state. The input gate i_t is expressed in Eq. (11).

$$i_t = \sigma(U_i x_t + W_i h_{t-1} + b_i) \quad (11)$$

Where U_i and W_i are the weight values. At time t, the o_t output gate adopts stored value in the c_t cell state and it is expressed in Eq. (12).

$$o_t = \sigma(U_o x_t + W_o h_{t-1} + b_o) \quad (12)$$

The c_t cell state at time t is expressed in Eq. (13).

$$c_t = i_t \circ a_t + f_t \circ c_{t-1} \quad (13)$$

Where at t time, a_t and $\circ$ are the new cell state and the product of element-wise correspondingly. The a_t is expressed in Eq. (14).

$$a_t = \tanh\,(U_c x_t + W_c h_{t-1} + b_c) \quad (14)$$

Finally, h_t the hidden state is expressed in Eq. (15).

$$h_t = o_t \circ \tanh(c_t) \quad (15)$$

3.5.2. Bidirectional long-short term memory (Bi-LSTM)

Bi-LSTM is a neural network utilizing LSTM approach for every bidirectional RNN hidden node. The outcome value is impacted by the hidden state and prior input values which is divided in the direction of forward and backward. The forward hidden state $\vec{h}_t$ at time t is expressed in Eq. (16).

$$\vec{h}_t = \sigma(U_{\rightarrow x_t} + W_{\rightarrow}\vec{h}_{t-1} + b_{\rightarrow}) \quad (16)$$

Where $U_{\rightarrow}$ and $W_{\rightarrow}$ are the value of weight and $b_{\rightarrow}$ is a bias value. At time t, the backward hidden state $\overleftarrow{h}_t$ is expressed in Eq. (17).

$$\overleftarrow{h}_t = \sigma(U_{\leftarrow x_t} + W_{\leftarrow}\overleftarrow{h}_{t+1} + b_{\rightarrow}) \quad (17)$$

The output y_t at time t is expressed in Eq. (18).

$$y_t = V_{\rightarrow}\vec{h}_t + V_{\leftarrow}\overleftarrow{h}_t + b_o \quad (18)$$

The brain tumor classification achieves better performance by using Bi-LSTM in this proposed approach.

4. Results

The proposed BT-Bi-LSTM is simulated employing a Python environment with 16GB RAM system configuration, Intel core i7 Processor, and Windows 10 Operating System. Precision, accuracy, f1-score, and recall are used to determine the proposed technique is indicated in Eqs. (19), (20), (21), and (22)

- Accuracy –It is the accurate detection proportion for every sample is computed utilizing Eq. (19)

$$Accuracy = \frac{TP+TN}{TN+TP+FN+FP} \times 100 \quad (19)$$

- Precision – It computes actual data records percentage vs expected records of data. Whether the precision is greater, the model's classification performance is greater using Eq. (20).

$$Precision = \frac{TP}{TP+FP} \quad (20)$$

- Recall –It is computed as sum of true positives and the positive image of class using Eq. (21)

$$Recall = \frac{TP}{TP+FN} \quad (21)$$

- F1-score – It is a harmonic mean that helps to balance among recall and precision using Eq. (22).

$$F1 - Score = \frac{2\times TP}{2\times TP+FP+FN} \times 100 \quad (22)$$

Where TP is True Positive, FP is False Positive, FN is False Negative, and TN is True Negative.

4.1 Qualitative and quantitative analysis

It represents quantitative and qualitative performance of BT-Bi-LSTM which is indicated in Tables 1 to 6. Table 1 represents the performance of segmentation by utilizing Bi-LSTM in BRATS 2019 dataset. The performance of global thresholding (GT), adaptive thresholding (AT), and otsu thresholding

Table 1. Performance of Segmentation using Bi-LSTM in BRATS 2019 dataset

Method	Accuracy (%)	Precision (%)	Recall (%)	F1-score (%)
GT	86.41	86.20	85.61	85.23
AT	88.69	87.45	87.12	86.93
OT	91.25	90.62	89.35	89.44
BT	93.21	92.36	91.69	90.53

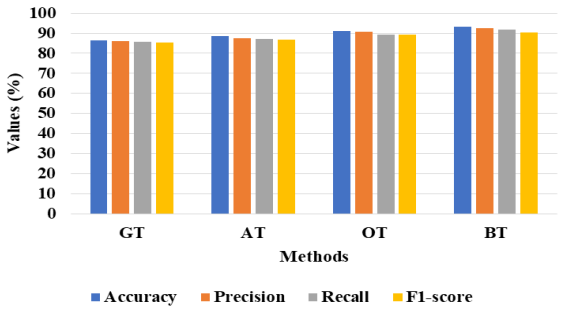

Figure. 2 Graphical representation of segmentation using BRATS 2019

(OT) are compared with BT approach. GT does not appropriate for images with the distribution of intricate intensity or when there is variation in condition of lighting across image. AT needs additional computational resources and sensitive to uneven illumination or noise with the image that affects entire segmentation performance. OT does not segment weak objects it searches for a single threshold to divide an image in two classes background and foreground. The proposed BT provides effectiveness in segmentation of image by adjusting threshold dynamically based on a value of local pixels which makes it robust in varying the condition of illumination and improves foreground and background separation accuracy. Fig. 2. shows the Graphical representation of segmentation using the BRATS 2019 dataset. The acquired outcomes indicate BT achieves accuracy of 93.21% that is better compared to the existing optimization approach.

Table 2 represents classification performances without segmentation utilizing BRATS 2019 dataset. The performance of DNN, RNN, CNN, and LSTM are compared with Bi-LSTM approach. Fig. 3. shows Graphical representation of classification without segmentation. The acquired outcomes represent Bi-LSTM approach achieves accuracy of 94.14% which is better when compared to existing optimization approaches.

Table 3 represents classification performances with segmentation utilizing BRATS 2019 dataset. The performance of DNN, RNN, CNN, and LSTM are compared with Bi-LSTM approach. Fig. 4. shows

Table 2. Performance of classification without segmentation using the BRATS 2019 dataset

Method	Accuracy (%)	Precision (%)	Recall (%)	F1-score (%)
RNN	88.20	87.85	87.12	86.14
CNN	89.54	88.67	87.74	87.96
LSTM	92.68	90.38	91.89	90.43
Bi-LSTM	94.14	93.75	93.17	93.33

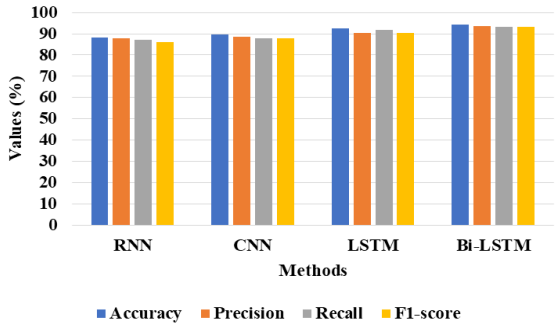

Figure. 3 Graphical representation of classification without segmentation using BRATS 2019

Table 3. Performance of classification with segmentation using BRATS 2019 dataset

Method	Accuracy (%)	Precision (%)	Recall (%)	F1-score (%)
RNN	95.25	95.03	95.15	94.26
CNN	97.68	96.38	96.27	97.58
LSTM	98.96	98.47	97.64	98.36
Bi-LSTM	99.76	99.52	99.31	98.69

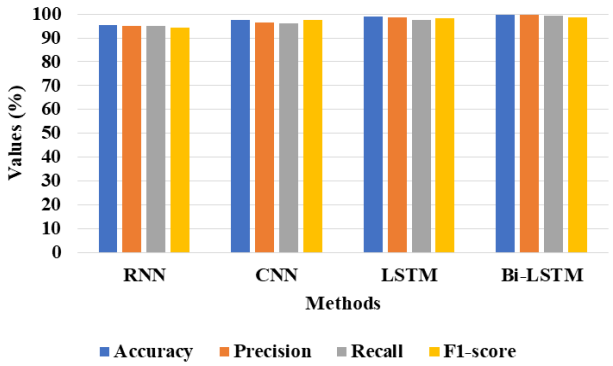

Figure. 4 Graphical representation of classification with segmentation using BRATS 2019

graphical representation of classification with segmentation. The acquired outcomes indicate Bi-LSTM approach achieves accuracy of 99.76% which is better compared to existing optimization approaches.

Table 4 indicate segmentation performance utilizing Bi-LSTM in BRATS 2020 dataset. The performance of GT, AT, and OT are compared with BT approach. Fig. 5. shows the Graphical

Table 4. Performance of Segmentation using Bi-LSTM in BRATS 2020 dataset

Method	Accuracy (%)	Precision (%)	Recall (%)
GT	87.58	86.48	86.22
AT	87.94	87.03	87.54
OT	88.24	88.47	87.17
BT	90.17	90.03	89.27

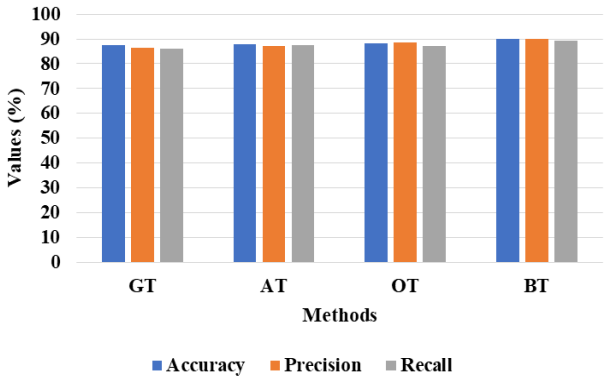

Figure. 5 Graphical representation of segmentation using BRATS 2020

Table 5. Performance of classification without segmentation using BRATS 2020 dataset

Method	Accuracy (%)	Precision (%)	Recall (%)
RNN	91.28	90.25	91.17
CNN	92.87	91.44	91.23
LSTM	93.65	92.58	92.58
Bi-LSTM	94.77	93.67	92.99

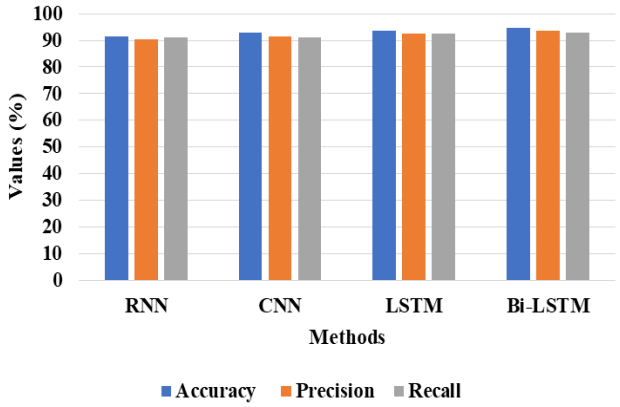

Figure. 6 Graphical representation of classification without segmentation using BRATS 2020

Table 6. Performance of classification with segmentation using BRATS 2020 dataset

Method	Accuracy (%)	Precision (%)	Recall (%)
RNN	96.25	95.47	95.02
CNN	97.36	96.25	96.14
LSTM	98.45	97.63	98.37
Bi-LSTM	99.89	99.76	99.62

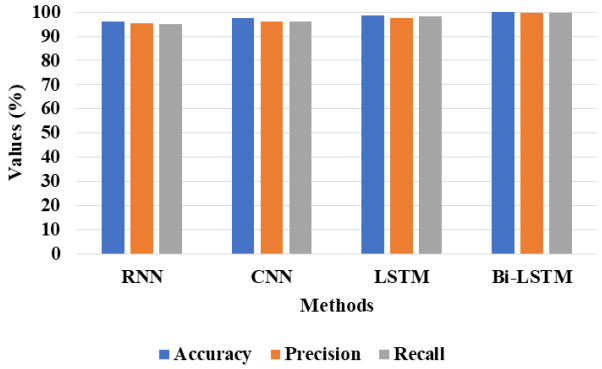

Figure. 7 Graphical representation of classification with segmentation using BRATS 2020

representation of segmentation using BRATS 2020 dataset. The acquired outcomes BT technique achieves accuracy of 90.17%, precision of 90.03%, and recall of 89.27% is better compared to existing optimization approaches.

Table 5 shows classification performance without segmentation employing BRATS 2020 dataset. The performance of DNN, RNN, CNN, and LSTM is compared with Bi-LSTM technique. Fig. 6. shows the Graphical representation of classification without segmentation. The acquired outcomes indicate Bi-LSTM achieves accuracy of 94.77%, precision of 93.67%, and recall of 92.99% which is better compared to existing optimization approaches.

Table 6 indicates classification performances with segmentation employing BRATS 2020 dataset. The performance of DNN, RNN, CNN, and LSTM are compared with Bi-LSTM. Fig. 7. shows Graphical representation of classification with segmentation. The acquired outcomes represent Bi-LSTM achieves accuracy of 99.89% which is better compared to existing optimization approaches.

4.2 Comparative analysis

Here, comparative analysis of proposed BT-Bi-LSTM using BRATS 2019 and BRATS 2020 is indicated in Tables 7 and 8. The existing methods like the DNN-based mathematical approach [16] and Tumor localization and enhancement approach and U-net architecture [17], and HCNN [19] are employed to evaluate the BT-Bi-LSTM approach for BRATS 2019 dataset. When compared to these existing techniques, the BT-Bi-LSTM achieves better accuracy, recall, precision, and f1-score of 99.76%, 99.31%, 99.52%, and 98.69% for BRATS 2019. The proposed BT-Bi-LSTM achieves accuracy, recall, and precision of 99.89%, 99.62%, and 99.76% for the BRATS 2020 dataset compared to the existing approaches like Tumor localization and enhancement approach and U-net architecture [17], CNN [18],

Table 7. Comparative Analysis of existing methods using BRATS 2019 dataset

Methods	Dataset	Accuracy (%)	Precision (%)	Recall (%)	F1-score (%)
DNN-based mathematical approach [16]	BRATS 2019	98.90	99	98	98.50
Tumor localization and enhancement approach and U-net architecture [17]		99.38	92.60	N/A	N/A
HCNN [19]		99.7	N/A	N/A	N/A
Proposed BT-Bi-LSTM		99.76	99.52	99.31	98.69

Table 8. Comparative Analysis of existing methods using BRATS 2020 dataset

Methods	Dataset	Accuracy (%)	Precision (%)	Recall (%)
Tumor localization and enhancement approach and U-net architecture [17]	BRATS 2020	99.40	92.94	N/A
CNN [18]		99.74	N/A	N/A
hybrid Deep CNN with k-means clustering [20]		99.09	N/A	N/A
2D U-net [21]		99.41	N/A	N/A
Proposed BT-Bi-LSTM		99.89	99.76	99.62

hybrid Deep CNN with k-means clustering [20], 2D U-net [21] respectively.

4.3 Discussion

The benefits of BT-Bi-LSTM and limitations of existing techniques are discussed. The existing DNN-based mathematical approach [16] has limited memory and false tolerance. CNN [18] has limitations such as time complexity and required weight approaches for different data fusions. HCNN [19] faces difficulties in interpretability because of the complexity of integrating various CNNs. The proposed BT-Bi-LSTM overcomes the existing techniques limitations. The BT effectively separates a regions of brain tumors from normal brain tissues depending on intensity distribution. It generates a straightforward and computationally effective model for describing tumor boundaries in medical images. Bi-LSTM makes the integration of both prior and future contextual data which provides more accurate tumor classification. It generates efficient modeling of long-range dependencies for determining intricate patterns in sequential data. The BT-Bi-LSTM achieves better accuracy of 99.76% and 99.89% for BRATS 2019 and BRATS 2020 datasets compared to the existing techniques like DNN-based mathematical approach, Tumor localization and enhancement approach and U-net architecture, CNN, HCNN, hybrid Deep CNN with k-means clustering, 2D U-net respectively.

5. Conclusion

In this research, BT-Bi-LSTM is proposed for brain tumor segmentation and classification. At first, image is acquired from both datasets and then pre-processing is employed to modify the pixel intensity and enhance the contrast and image's features by declaring the abnormal patterns. The BT approach is used to segment the tumor portions from the images. The GLCM and LTP approach is established to extract the features from the segmented images. Finally, Bi-LSTM is employed to classify brain tumor types effectively and accurately. The proposed BT-Bi-LSTM achieves better accuracy of 99.76% and 99.89% for BRATS 2019 and BRATS 2020 datasets compared to the existing techniques like DNN-based mathematical approach, Tumor localization and enhancement approach and U-net architecture, CNN, HCNN, hybrid Deep CNN with k-means clustering, 2D U-net respectively. In the future, the segmentation and classification of brain tumors will be analyzed using huge datasets.

Conflicts of interest

The authors declare no conflict of interest.

Author contributions

The paper conceptualization, methodology, software, validation, formal analysis, investigation, resources, data curation, writing—original draft preparation, writing—review and editing, visualization, the supervision and project administration, have been done by 1st author.

Table notation

Symbol	Description
I	input image
max and min	maximum and minimum intensity values
I'	normalized image with $newmin$ and $newmax$ value
G	grey levels
$N_n(x, y)$	normalized image
I_a	the pixels at specific grey levels
$\mu\ (t_1)$	mean
$\sigma_c^2(t_1)$	binomial variance
$P_c(t_1)$	cumulative probability
$\tilde{\phi}^T$	threshold value
t	subject threshold
x_t and h_t	input and the hidden state
c_t	cell state
f_t	forget gate
i_t	input gate
o_t	output gate
c_{t-1}	prior cell state
σ	function of the sigmoid
W_f and U_f	weight values
b_i	bias value
a_t and $\circ$	new cell state
h_t	hidden state
$\vec{h}_t$	forward hidden state
$U_{\rightarrow}$ and $W_{\rightarrow}$	Weight values
$\overleftarrow{h}_t$	backward hidden state
y_t	output

References

[1] H. Habib, R. Amin, B. Ahmed, and A. Hannan, "Hybrid algorithms for brain tumor segmentation, classification and feature extraction", *Journal of Ambient Intelligence and Humanized Computing*, pp. 1-22, 2021.

[2] S. Z. Kurdi, M. H. Ali, M. M. Jaber, T. Saba, A. Rehman, and R. Damaševičius, "Brain Tumor Classification Using Meta-Heuristic Optimized Convolutional Neural Networks", *Journal of Personalized Medicine*, Vol. 13, No. 2, p. 181, 2023.

[3] M. O. Khairandish, M. Sharma, V. Jain, J. M. Chatterjee, and N. Z. Jhanjhi, "A hybrid CNN-SVM threshold segmentation approach for tumor detection and classification of MRI brain images", *Irbm*, Vol. 43, No. 4, pp. 290-299, 2022.

[4] H. Kibriya, M. Masood, M. Nawaz, and T. Nazir, "Multiclass classification of brain tumors using a novel CNN architecture", *Multimedia Tools and Applications*, Vol. 81, No. 21, pp. 29847-29863, 2022.

[5] P. Agrawal, N. Katal, and N. Hooda, "Segmentation and classification of brain tumor using 3D-UNet deep neural networks", *International Journal of Cognitive Computing in Engineering*, Vol. 3, pp. 199-210, 2022.

[6] R. Pitchai, P. Supraja, A. H. Victoria, and M. J. N. P. L. Madhavi, "Brain tumor segmentation using deep learning and fuzzy K-means clustering for magnetic resonance images", *Neural Processing Letters*, Vol. 53, pp. 2519-2532, 2021.

[7] R. Kalam, C. Thomas, and M. A. Rahiman, "Brain tumor detection in MRI images using adaptive-ANFIS classifier with segmentation of tumor and edema", *Soft Computing*, Vol. 27, No. 5, pp. 2279-2297, 2023.

[8] T. Balamurugan and E. Gnanamanoharan, "Brain tumor segmentation and classification using hybrid deep CNN with LuNetClassifier", *Neural Computing and Applications*, Vol. 35, No. 6, pp. 4739-4753, 2023.

[9] S. Kumar and D. Kumar, "Human brain tumor classification and segmentation using CNN", *Multimedia Tools and Applications*, Vol. 82, No. 5, pp. 7599-7620, 2023.

[10] S. Deepa, J. Janet, S. Sumathi, and J. P. Ananth, "Hybrid Optimization Algorithm Enabled Deep Learning Approach Brain Tumor Segmentation and Classification Using MRI", *Journal of Digital Imaging*, Vol. 36, No. 3, pp. 847-868, 2023.

[11] K. Swaraja, K. Meenakshi, H. B. Valiveti, and G. Karuna, "Segmentation and detection of brain tumor through optimal selection of integrated features using transfer learning", *Multimedia Tools and Applications*, Vol. 81, No. 19, pp. 27363-27395, 2022.

[12] S. Preethi and P. Aishwarya, "An efficient wavelet-based image fusion for brain tumor detection and segmentation over PET and MRI image", *Multimedia Tools and Applications*, Vol. 80, No. 10, pp. 14789-14806, 2021.

[13] P. Sathish and N. M. Elango, "Gaussian hybrid fuzzy clustering and radial basis neural network for automatic brain tumor classification in MRI images", *Evolutionary Intelligence*, Vol. 15, No. 2, pp. 1359-1377, 2022.

[14] S. M. Kurian and S. Juliet, "An automatic and intelligent brain tumor detection using Lee sigma filtered histogram segmentation model", *Soft Computing*, Vol. 27, No. 18, pp. 13305-13319, 2023.

[15] I. Aboussaleh, J. Riffi, A. M. Mahraz and H. Tairi, "Brain tumor segmentation based on deep learning's feature representation", *Journal of Imaging*, Vol. 7, No. 12, p. 269, 2021.

[16] A. S. Ladkat, S. L. Bangare, V. Jagota, S. Sanober, S. M. Beram, K. Rane, and B. K. Singh, "Deep neural network-based novel mathematical model for 3D brain tumor segmentation", *Computational Intelligence and Neuroscience*, Vol. 2022, 2022.

[17] A. Ilhan, B. Sekeroglu, and R. Abiyev, "Brain tumor segmentation in MRI images using nonparametric localization and enhancement methods with U-net", *International Journal of Computer Assisted Radiology and Surgery*, Vol. 17, No. 3, pp. 589-600, 2022.

[18] A. Chattopadhyay and M. Maitra, "MRI-based brain tumour image detection using CNN based deep learning method", *Neuroscience Informatics*, Vol. 2, No. 4, p. 100060, 2022.

[19] B. V. Prakash, A. R. Kannan, N. Santhiyakumari, S. Kumarganesh, D. S. S. Raja, J. J. Hephzipah, K. MartinSagayam, M. Pomplun and H. Dang, "Meningioma brain tumor detection and classification using hybrid CNN method and RIDGELET transform", *Scientific Reports*, Vol. 13, No. 1, p.14522, 2023.

[20] A. K. Sahoo, P. Parida and K. Muralibabu, "Hybrid deep neural network with clustering algorithms for effective gliomas segmentation", *International Journal of System Assurance Engineering and Management*, pp. 1-17, 2023.

[21] S. Montaha, S. Azam, A. K. M. R. H. Rafid, M. Z. Hasan and A. Karim, "Brain Tumor Segmentation from 3D MRI Scans Using U-Net", *SN Computer Science*, Vol. 4, No. 4, p. 386, 2023.

[22] BRATS 2019 dataset link: https://www.kaggle.com/datasets/aryashah2k/brain-tumor-segmentation-brats-2019/data.

[23] BRATS 2020 dataset link: https://www.kaggle.com/datasets/awsaf49/brats2020-training-data.

[24] R. Vankdothu and M. A. Hameed, "Brain tumor MRI images identification and classification based on the recurrent convolutional neural network", *Measurement: Sensors*, Vol. 24, p. 100412, 2022.

[25] D. Ndayikengurukiye and M. Mignotte, "Salient object detection by ltp texture characterization on opposing color pairs under slico superpixel constraint", *Journal of Imaging*, Vol. 8, No. 4, p. 110, 2022.